ISSN : 0974 - 746X Volume 5 Issue 2

Inorganic CHEMISTRY

An Indian Journal

Full Paper

ICAIJ, 5(2), 2010 [000-000]

Synthesis, structural characterisation, thermal properties and bacterial activity of bimetallic bis(dithiocarbamate)-based macrocyclic complexes

Enaam I.Yousif, Hasan A.Hasan, Riyadh M.Ahmed, Mohamad J.Al-Jeboori*

Department of Chemistry, College of Education for Pure Science (Ibn Al-Haitham),University of Baghdad, P.O. Box 4150, Adhamiyah, Baghdad,(IRAQ)

E-mail : mohamadaljeboori@yahoo.com

ABSTRACT

A range of new binuclear metal(II) dithiocarbamate-based macrocyclic complexes is reported. The formation of complexes was achieved either by the reaction of the free ligand with a metal ion or via a one-pot reaction. The preparation of the bis-amine precursors (A and B) was achieved through several synthetic routes. The reaction of bis-amine precursor with CS_2 in presence of KOH yielded in the formation of free ligand namely; potassium 2,2'-(biphenyl-4,4'-diylbis(azanediyl)) bis(1-chloro-2-oxoethane-2,1-diyl) bis(cyclohexylcarbamodithioate) (L^1) and potassium 2,2'-(biphenyl-4,4'-diylbis(azanediyl)) bis(1-chloro-2-oxoethane-2,1-diyl) bis(isopropyl-carbamodithioate) (L^2). Physico-chemical techniques were used to characterised ligands and their complexes. These include; elemental analysis, thermal properties, FTIR, UV-Vis, mass spectroscopy, magnetic susceptibility, conductance, melting points, and ^1H, ^{13}C-NMR spectroscopy. These studies indicated the preparation of binuclear macrocyclic complexes of the general formulae $[M(L^n)]_2$ (M= Mn^{II}, Co^{II}, Ni^{II}, Cu^{II}, Zn^{II} and Cd^{II}; n = 1 or 2) with tetrahedral arrangement for Mn^{II}, Co^{II}, Zn^{II} and Cd^{II}, and square planar geometries with Ni^{II} and Cu^{II} complexes. Bacterial activity of the ligands and their metal complexes were tested against four bacterial species *(Escherichia coli, Pseudomonas aeruginosa, Staphylococcus aureus and Bacillus stubtilis)*, which indicated that the complexes are potentially more active against these bacterial strains, compared with the free ligands.

KEYWORDS

Bis(dithiocarbamate) macrocyclic complexes;
One-pot reaction;
Structural studies;
Thermal properties;
Bacterial activity.

INTRODUCTION

Dithiocarbamates are versatile compounds that have shown a range of applications. These species played a key role in the development of chemistry, due to their importance in synthetic inorganic[1], bioinorganic[2], analytical[3] and environmental chemistry[4]. Dithiocarbamates (DTCs) is flexible ligands that have the ability to bind transition and representative elements. The importance of dithiocarbamates (DTCs) is due to their ability to stabilise metal ion in a range of oxidation states. This is related to their strongly chelating ability

towards metal ions. Further, upon complexation, these species permitting the metal ion to adopt its most preferable geometry[5]. The presence of the anionic CS_2^- moiety allowed DTCs molecules to achieve a range of binding modes; monodentate, bidentate or bridging, upon complexation[6-8]. Dithiocarbamates are essential materials that have been extensively investigated with regard to their numerous applications in coordination chemistry[1], materials science[9], medicine and radiopharmaceutical chemistry[10,11], sensing technology[12] and in the industry[13]. More, the act of dithiocarbamates against some tumours, fungi, bacteria, and other microorganisms[14,15] make them a hot topic for several research groups. In this paper, we report the preparation, structural characterisation, thermal analysis and bacterial activity of new DTCs ligands and their macrocyclic metal-based complexes.

EXPERIMENTAL

Materials

All reagents were commercially available and used without further purification. Solvents were distilled from appropriate drying agents immediately prior to use.

Physical measurements

Elemental analyses (C, H, N and S) for ligands and their metal complexes were carried out on a Euro EA 3000. Melting points were obtained on an Electrothermal Stuart SMP40 melting point apparatus and are uncorrected. FT-Infrared spectra were obtained as KBr discs using a Shimadzu 8300s FT-IR spectrophotometer in the range 4000-400 cm^{-1} and as CsI discs in the range 400-200 cm^{-1}. Electronic spectra were measured between 200-1100 nm with 10^{-3} M solutions in dimethylsulfoxide (DMSO) spectroscopic grade solvent at 25 °C using a Perkin-Elmer spectrophotometer Lambda. Thermogravimetric analysis was carried out using an STA PT-1000 Linseis company /Germany. Mass spectra were obtained by positive Electrospray mass spectroscopy technique (ESMS). NMR spectra (^1H, ^{13}C-NMR) were acquired in DMSO-d_6 solutions using a Brucker-300 for ^1H-NMR and 75 MHz for ^{13}C-NMR, respectively with tetramethylsilane (TMS) for ^1H NMR. Metals were determined using a Shimadzu (A.A) 680 G atomic absorption spectrophotometer. Conductivity measurements were made with DMSO solutions using a Jenway 4071 digital conductivity metre at room temperature. Magnetic moments were measured with a magnetic susceptibility balance (Sherwood Scientific).

SYNTHESIS

Preparation of the bis-amine precursors (A and B)

A standard method reported in[16,17] was used for the preparation of the precursors (A and B). The free bis-amine precursors were prepared by two steps, and as follows:

(1) Preparation of N,N'-(biphenyl-4,4'-diyl)bis(2-dichloroacetamide)

To a mixture of benzidine (2.16g, 11.72mmol) dissolved in $CHCl_3$ (50mL), was added with stirring potassium hydroxide (1.32g, 23.44mmol) in H_2O (20mL). Dichloroacetyl chloride (3.45g, 23.44mmol) dissolved in $CHCl_3$ (50mL) was added dropwise with stirring to the above mixture. After 15 minutes a white precipitate that formed was filtered off and then washed with Et_2O (20mL). The collected white solid was air-dried, m.p=235-237 °C. Yield: 4.51g, (94%). FTIR (cm^{-1}), 3249 ν(-CON-H), 1674 ν(C=O), 1606 δ(N-H), 1529 ν_{ar}(C=C). The electrospray (+) mass spectrum of the N,N'-(biphenyl-4,4'-diyl)bis(2-dichloroacetamide) exhibited the parent ion peak at *m/z* = 406.1$(M)^+$(28%) for $C_{16}H_{12}Cl_4N_2O_2$; requires =406.09 and the following fragments; 280.2 (40%) and 154.2 (13%) correspond to $[M-(NH-CO-CHCl_2)]^+$ and $[M-(NH-CO-CHCl_2)+(NH-CO-CHCl_2)]^+$, respectively (see supporting information, Figure SI 1). NMR data (ppm), δ_H(300 MHz, DMSO-d_6): 8.63 (2H, s, N-*H*), 7.68, 7.69 (4H, d, J_{HH}= 2.1 Hz), 7.40, 7.41 (4H, d, J_{HH}= 2.4 Hz) ($C_{4,4'}$, $_{6,6'}$-*H*) ($C_{5,5'}$, $_{7,7'}$-*H*)Ar-*H*, 6.69-6.70 (2H, s,$CHCl_2$) ($C_{1,1'}$-*H*) (see supporting information, Figure SI 8); δ_C(75MHz, DMSO-d_6): 59.90 ($CHCl_2$, $2C_1$), 120.26 and 126.81 (Ar-$C_{4,5,6,7}$), 161.32 ($2C_2$=O) (see supporting information, Figure SI 9).

(2) Preparation of bis-amine N,N'-(biphenyl-4,4'-diyl)bis(2-(cyclohexylamine) chloroacetamide) (A) and bis-amine N,N'-bis(2- (Isopropyl amino chloroacetamide-4,4-diamine]dibenzene (A)

An excess of cyclohexylamine (3.90g, 39.40mmol)

was heated up to 40 ºC, and then N,N'-(biphenyl-4,4'-diyl)bis(2-dichloroacetamide) (4.00g, 9.85mmol) was added portion-wise with stirring. The mixture was stirred at 40 ºC for 12 h, and then H_2O (200mL) was added. The product was extracted into CH_2Cl_2 (4 x 50 mL), washed with H_2O (200mL) and dried over K_2CO_3. Solvent was removed under reduced pressure and brown oil was obtained. 2.86g (54 %). FTIR cm^{-1}, 3342 ν(N-H), 3222 ν(-CON-*H*), 3032 ν_{ar}(C-H), 2929 and 2858 ν_{ali}(C-H), 1676 ν(C=O), 1622 δ(N-H), 1498 ν_{ar}(C=C), 700 ν (C-Cl). The electrospray (+) mass spectrum of the bis-amine showed the parent ion peak at *m/z* =532.2 $(M+H)^+$ (7%) for $C_{26}H_{36}Cl_2N_4O_2$, requires =531.52 and the following fragments at *m/z* =343.9 (16%), 260.8 (90%) and 154.3 (14%), corresponding to $[M-(C_6H_6\text{-}NH\text{-}Cl\text{-}CO\text{-}NH)]^+$, $[M-(C_6H_6\text{-}NH\text{-}Cl\text{-}CO\text{-}NH)+(C_6H_6)]^+$ and $[M-(C_6H_6\text{-}NH\text{-}Cl\text{-}CO\text{-}NH)+(C_6H_6)+(NH_2\text{-}Cl\text{-}CO\text{-}NH)]^+$, respectively (see supporting information, Figure SI 2). NMR data (ppm), δ_H(300 MHz, DMSO-d_6): 1.09-1.25 (8H, q, J_{HH}=4.8Hz,($C_{B,B'\,F,F'}$-*H*)), 1.48-1.52 (12H, m, ($C_{C,C',D,D',E,E'}$-*H*)), 3.16-3.17 (2H, m, ($C_{A,A'}$-*H*)), 3.91 (2H, t, NH), 5.38 (2H, d, J_{HH}=2.1Hz, ($C_{1,1'}$-*H*)), 8.87 (2H, s, amidic-*H*), 7.59 (4H, d, J_{HH}=6.3Hz, ($C_{4,4',6,6'}$-*H*)), 7.54 (4H, d, J_{HH}=6.8Hz, ($C_{5,5',7,7'}$-*H*)) (Aromatic-H), (see supporting information, Figure SI 10); δ_C (75 MHz, DMSO-d_6): 23.90 ($C_{B,B'\,F,F'}$-*H*), 25.16 ($C_{C,C',E,E'}$-*H*), 31.97 ($C_{D,D'}$), 56.30 ($C_{A,A'}$), 79.18 ($C_{1,1'}$), 119.65 ($C_{4,4',6,6'}$), 131.31 ($C_{5,5',7,7'}$), 163.64 (C=O, ($C_{2,2'}$)) (see

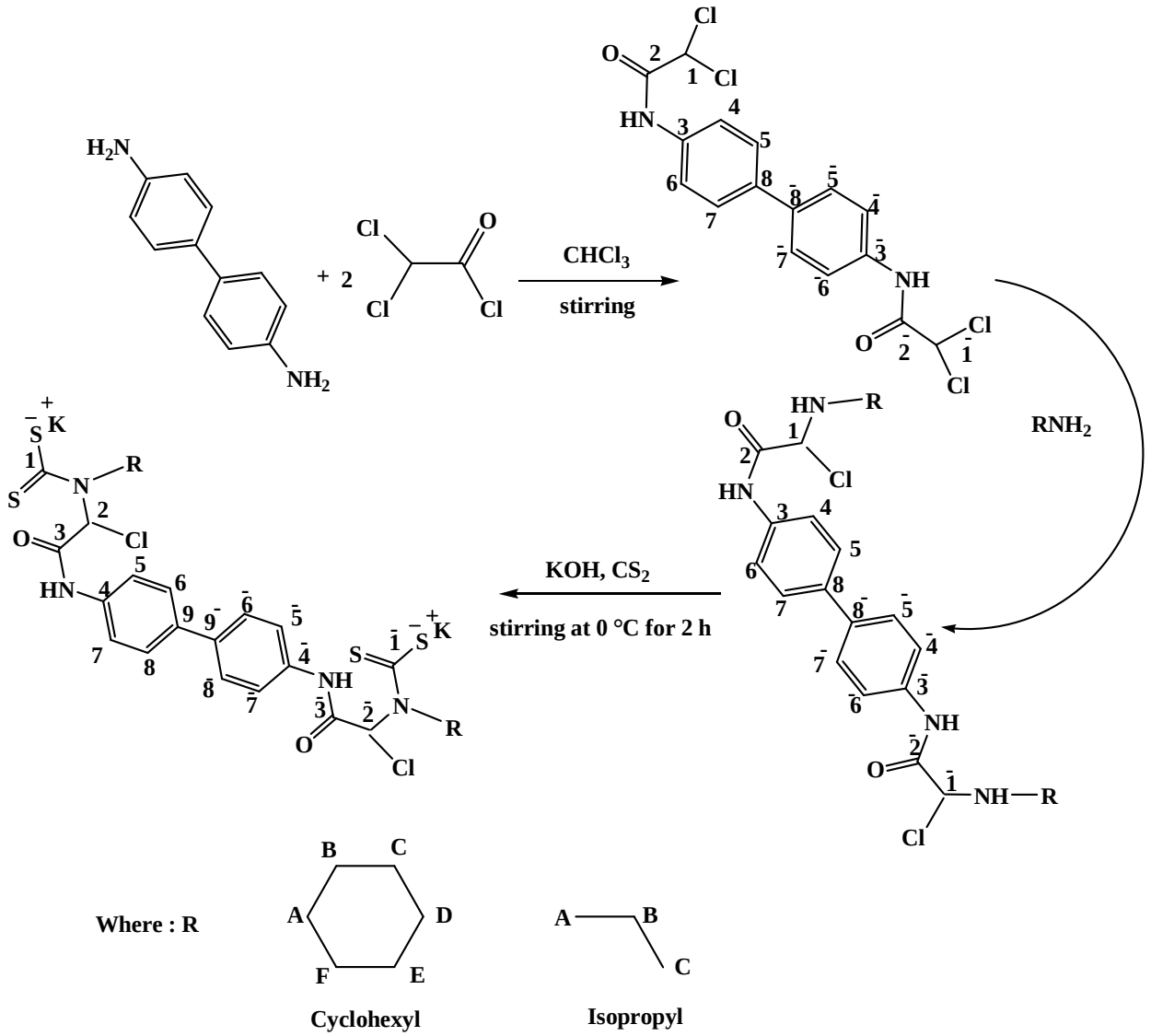

Scheme 1 : Synthetic route for ligands L^1 and L^2

Full Paper

supporting information, Figure SI 11).

The method used to prepare the secondary bis-amine (B) was analogues to that for (A), but with isopropylamine in place of cyclohexylamine. The quantities of the other reagent were adjusted accordingly. An identical work-up procedure gave the required compound as a dark orange solid. Yield: 2.67g, (60%). FTIR (cm^{-1}), 3332 ν(N-H), 3219 ν(-CON-*H*), 3032 ν_{ar}(C-H), 1664 ν(C=O), 1612 δ(N-H), 1498 ν_{ar}(C=C),742 ν (C-Cl). The electrospray (+) mass spectrum of the bis-amine showed the parent ion peak at *m/z*=451.6 $(M)^+$ (7%) for $C_{22}H_{26}Cl_2N_4O_2$, requires =451.39 and the following fragments at *m/z* =367.6 (50%), 261.4 (8%) and 154.6 (9%), corresponding to $[M-(CH_3\text{-}C\text{-}CH_3)_2]^+$, $[M-(CH_3\text{-}C\text{-}CH_3)_2+(NH_2\text{-}C\text{-}Cl\text{-}CO\text{-}NH)]^+$ and $[M-(CH_3\text{-}C\text{-}CH_3)_2+(NH_2\text{-}C\text{-}Cl\text{-}CO\text{-}NH)+(NH_2\text{-}C\text{-}Cl\text{-}CO\text{-}NH)]^+$ (see supporting information, Figure SI 3). NMR data (ppm), δ_H(300 MHz, DMSO-d_6): 3.44-3.45 (2H, d, J_{HH}=3 Hz), 1.46 -1.51 (12H, d, J_{HH}=16.2 Hz, ($C_{A,A'C,C'}$-*H*)), 2.58 -2.60 (2H, m,$C_{B,B'}$-*H*), 6.54 -6.56 (2H, d, J_{HH}=5.1 Hz, ($C_{1,1'}$-*H*)), 7.16-7.18 (4H, d, J_{HH}=6.3 Hz, $C_{4,4',6,6'}$-*H*), 7.59 -7.60 (4H, d, J_{HH}=3 Hz, $C_{5,5',7,7'}$-*H*), 8.27 (2H, s, amidic-*H*), (see supporting information,

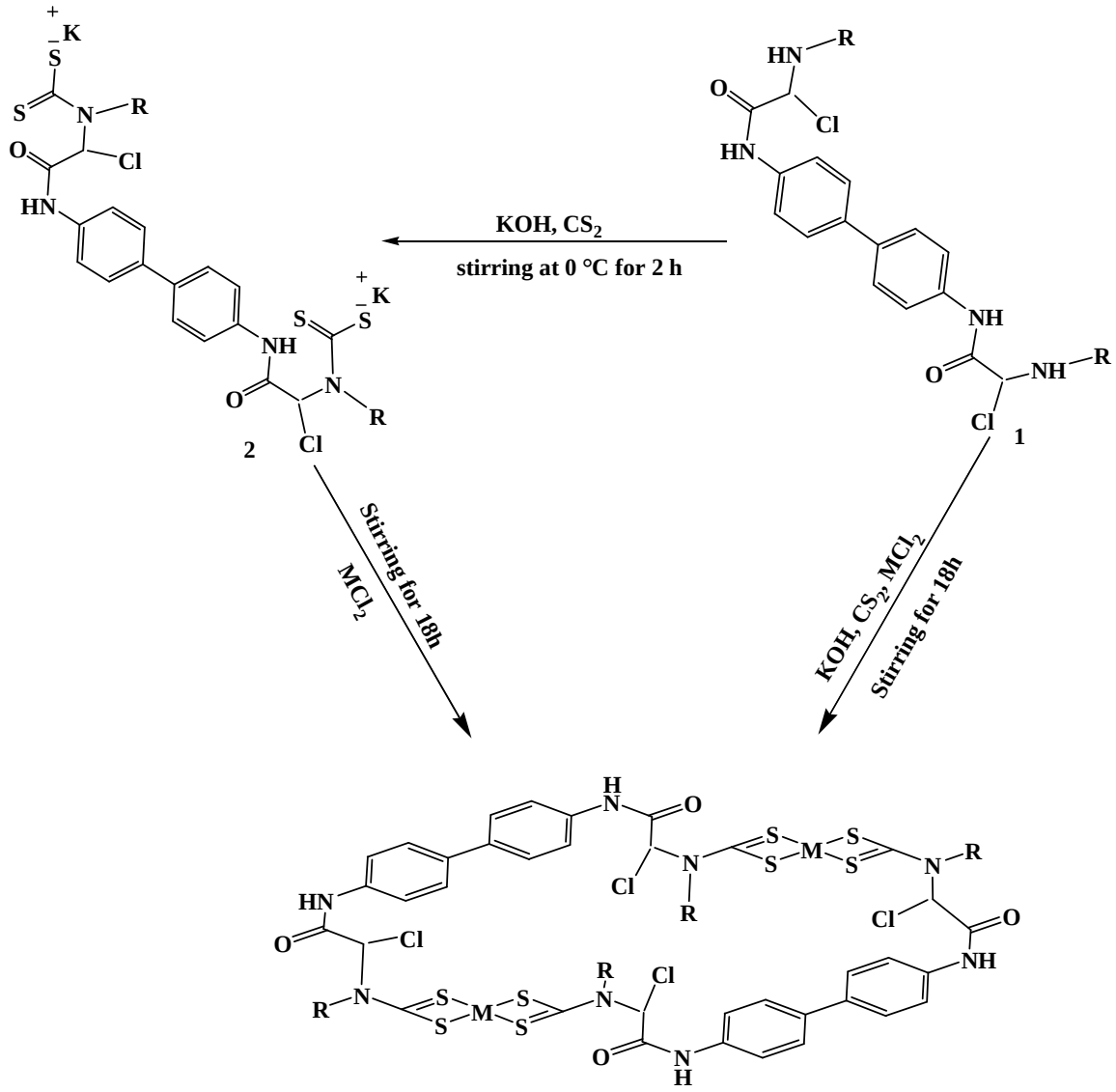

Where: R = Cyclohxyl = L^1 ; R = Isopropyl = L^2

M = Mn^{II}, Co^{II}, Ni^{II}, Cu^{II}, Zn^{II} and Cd^{II}

Scheme 2 : Synthetic route of macrocyclic complexes; a one pot approach; (2) from free ligand

Figure SI 12); δ_C (75 MHz, DMSO-d_6): 22.25 ($C_{A,A}$‘, $_{C,C}$‘), 51.07 ($C_{B,B}$‘), 79.81($C_{1,1}$‘), 114.20 ($C_{4,4}$‘ $_{,6,6}$‘), 126.60 ($C_{5,5}$‘ $_{,7,7}$‘), 163.35 (C=O)($C_{2,2}$‘), (see supporting information, Figure SI 13).

Synthesis of free ligands

Ligands were obtained according to conventional methods used in the preparation of dithiocarbamte compounds[18] as follows:

(1) Potassium2,2'- (biphenyl-4,4'-diylbis(azanediyl)) bis(1-chloro-2-oxoethane-2,1-diyl) bis (cyclohexylcarbamodithioate) (L^1)

An excess of KOH (0.126g, 2.25mmol, 4eq) dissolved in H_2O (2mL) was added with stirring to a solution of N, N'-(biphenyl-4,4'-diyl)bis(2-(cyclohexylamine) chloroacetamide) (0.30g, 0.56mmol) in 10 mL of a mixture of MeCN:H_2O (9:1). The mixture was placed in an ice bath, and then a solution of CS_2 (0.128g, 1.69mmol, 3eq) was added dropwise with stirring. The reaction mixture was kept at 0 °C for 2 h, and then potassium dithiocarbamate salt was collected as a light yellow solid, m. p=188-190 °C. Yield: 0.28g, (66%). FTIR cm^{-1}, 3299 ν(-CON-*H*), 3086 ν_{ar}(C-H), 1676 ν(C=O), 1622 δ(N-H) 1545, ν_{ar}(C=C), 1441ν(N-CS_2), 1084, 976 $\nu_{as,\,s}$ (CS_2) 654ν (C-Cl) (see supporting information, Figure SI 18). The electrospray (+) mass spectrum of the L^1 showed the parent ion peak at *m/z*=760.4 $(M+H)^+$ (14%) for $C_{30}H_{34}Cl_2K_2N_4O_2S_4$; requires =759.98 and the following fragments at *m/z*=681.6(12%), 529.7(8%), 341.5(55%) and 153.8 (7%) corresponding to $[M-(K)_2]^+$, $[M-(K)_2+(CS_2)_2]^+$, $[M-(K)_2+(CS_2)_2+(NH-CO-CHCl-N-C_6H_{11})]^+$ and $[M-(K)_2+(CS_2)_2+(NH-CO-CHCl-N-C_6H_{11})+(NH-CO-CHCl-N-C_6H_{11})]^+$ (see, supporting inform- ation, Figure SI 4). respectively. NMR data (ppm), δ_H(300 MHz, DMSO-d_6): 1.79-1.83 (2H, m, $C_{A,A}$‘-*H*), 1.50-1.60 (8H, q, J_{HH}=3 Hz, $C_{B,B}$‘ $_{F,F}$‘-*H*), 1.13-1.19 (12H, m, $C_{C,C}$‘ $_{,D,D}$‘ $_{,E,E}$‘-*H*), 5.01-5.02 (2H, s, ($C_{2,2}$‘-*H*)) 7.81-7.82 (4H, d, J_{HH}=2.1 Hz, $C_{4,4}$‘ $_{,6,6}$‘-*H*), 7.13-7.14 (4H, d, J_{HH}=2.7

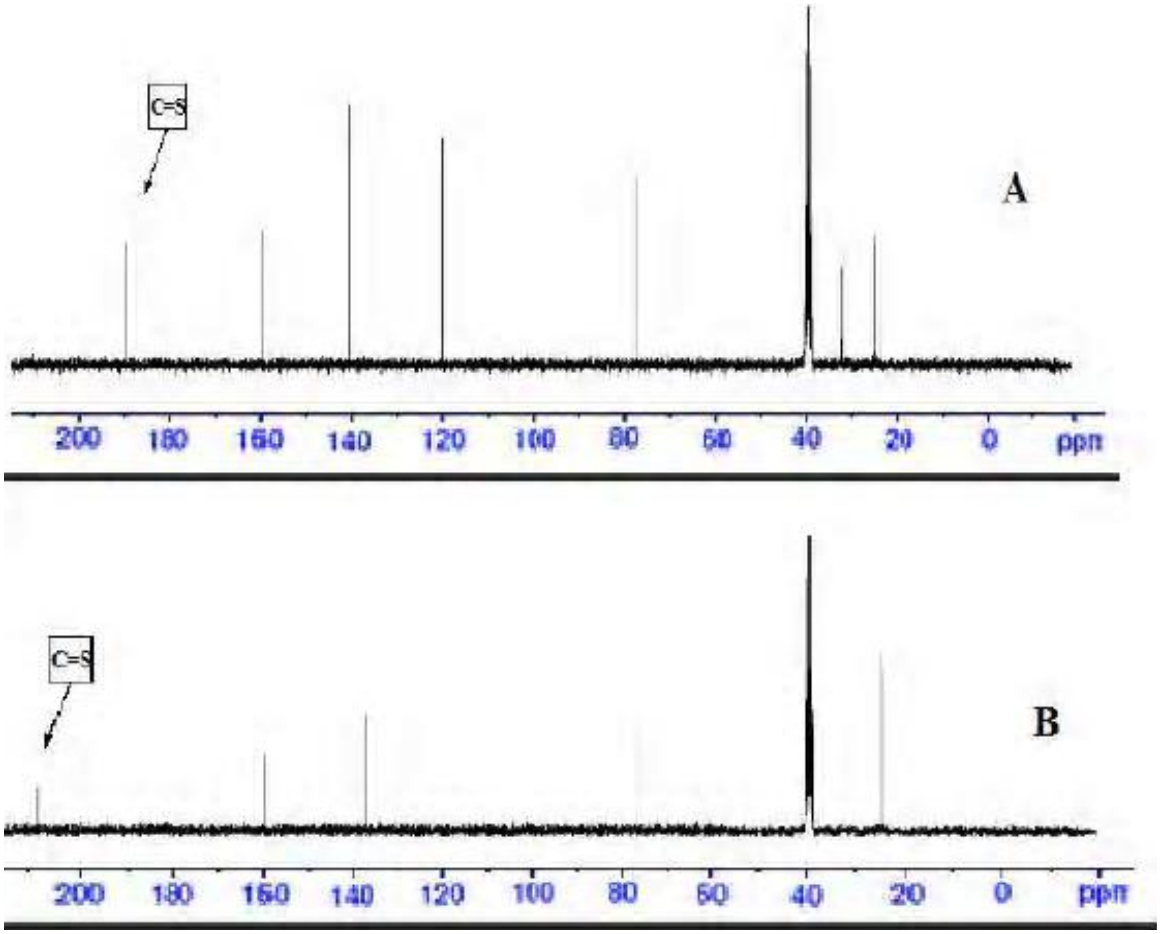

Figure 1 : ^{13}C NMR spectra in DMSO-d_6 solutions for: A) L^1; B) $[Cd(L^1)]_2$

Hz, ($C_{5,5'}$,$_{7,7'}$-*H*))(Ar-H), 8.45 (2H, s, amidic-*H*) (see supporting information, Figure SI 14); δ_C (75 MHz, DMSO-d_6): 24.457 ($C_{C,C'}$ $_{E,E'}$), 25.17 ($C_{D,D'}$), 32.32 ($C_{B,B'}$,$_{F,F'}$), 77.84 ($C_{2,2'}$), 119.95 ($C_{4,4'}$,$_{6,6'}$), 128.76 ($C_{5,5'}$,$_{7,7'}$), 160.33 (C=O) ($C_{3,3'}$), 189.87 (C=S) ($C_{1,1'}$) (see, Figure 1A).

(2) Synthesis of potassium 2,2'-(biphenyl-4,4'-diylbis(azanediyl))bis(1-chloro-2-oxoethane-2,1-diyl) bis(isopropylcarbamodithioate) (L^2)

The method that used to prepared L^2 was analogous to that for L^1, but with N, N'-[bis(2- (isopropyl amino chloroacetamide-4,4-diamine]dibenzene (0.30g, 0.66mmol) in place of N,N'-(biphenyl-4,4'-diyl)bis(2-(cyclohexylamine) chloroacetamide). A light orange solid was collected, m. p=173-175°C. Yield: 0.277g, (61.41%). FTIR cm^{-1}, 3259 ν(-CON-*H*), 3032 ν_{ar}(C-H), 1643 ν(C=O), 1529 ν_{ar}(C=C), 1498 ν(N-CS_2), 1001, 885 $\nu_{as,s}$(CS_2), 706 ν(C-Cl) (see TABLE (2) and supporting information, Figure SI 22). The electrospray (+) mass spectrum of the L^2 showed the parent ion peak at *m/z*=680.9 $(M+H)^+$, (13%) for $C_{24}H_{26}Cl_2K_2N_4O_2S_4$; requires=679.85 (see supporting information, Figure SI 5). NMR data (ppm), δ_H(300 MHz, DMSO-d_6): 1.80-1.83 (2H, m, ($C_{B,B'}$-*H*), 1.61, 1.63 (6H,d, J_{HH}=6.3Hz, ($C_{A,A'}$,$_{C,C'}$-*H*), 4.93 (2H, s, ($C_{2,2'}$-*H*), 7.46 (4H, t, J_{HH}=12 Hz, ($C_{E,E'}$-*H*), 7.58 (4H, t, J_{HH}=5.1 Hz, ($C_{F,F'}$,$_{G,G'}$-*H*), 7.54-7.55 (4H, d, J_{HH}=2.7 Hz, $C_{4,4'}$,$_{6,6'}$-*H*), 7.11-7.12 (4H, d, J_{HH}=2.4 Hz, $C_{5,5'}$,$_{7,7'}$-*H*) (Ar-H), 8.85 (2H, s, amidic-H) (see supporting information, Figure SI 15); δ_C(75 MHz, DMSO-d_6): 8.85 ($C_{A,A'}$,$_{C,C'}$), 55.43 ($C_{B,B'}$), 79.75 ($C_{2,2'}$) 119.68 ($C_{4,4'}$,$_{6,6'}$), 126.57 ($C_{5,5'}$,$_{7,7'}$), 163.26 (C=O) ($C_{3,3'}$), 190.346 (C=S) ($C_{1,1'}$) (see supporting information, Figure SI 16).

General method for synthesis of macrocyclic complexes

The bimetallic dithiocarbamate-based macrocyclic complexes were synthesised using standard methods reported in[19,20] using two approaches; (i) from the reaction of the free ligand with a metal ion, and (ii) via a one-pot reaction.

(1) Synthesis of macrocyclic complexes from free ligand

Complexes were prepared by the reaction of 1mmole of potassium dithiocarbamate salt, dissolved in 20mL of MeCN/H_2O (9:1) with 1 mmole of the metal salt; Mn^{II}, Co^{II}, Ni^{II}, Cu^{II}, Zn^{II} and Cd^{II}. The reaction mixture was stirred overnight, and distilled water was added, if necessary, to precipitate the product. The formed solid was filtered off, washed with methanol to give the macrocyclic complex. Elemental analysis data, colours and yields for the complexes are given in (TABLE1).

The ^{1}H-NMR data (ppm) for $[Cd(L^1)]_2$ complex, δ_H(300 MHz, DMSO-d_6): 1.83-1.84 (2H, m, $C_{A,A'}$-*H*), 1.58 (8H, t, J_{HH}=16.1 Hz, $C_{B,B'}$,$_{F,F'}$-*H*), 1.10-1.16 (12H, m, $C_{C,C'}$-$_{D,D'}$-$_{E,E'}$-*H*), 4.09 (2H, s, $C_{2,2'}$-*H*), 7.70-7.72 (4H, d, J_{HH}=8.1Hz, C $C_{4,4'}$,$_{6,6'}$-*H*), 6.87-6.91 (4H, d, J_{HH}=12.3 Hz, $C_{5,5'}$,$_{7,7'}$-*H*), 8.19 (2H, s, NH) (see supporting information, Figure SI 17). The ^{13}C-NMR spectrum for the $[Cd(L^2)]_2$, δ_C(75 MHz, DMSO-d_6): 25.23 ($C_{B,B'}$ $_{F,F'}$), 25.63 ($C_{D,D'}$), 32.14 ($C_{C,C'}$,$_{E,E'}$), 76.99($C_{2,2'}$), 118.996 ($C_{4,4'}$,$_{6,6'}$), 127.87 ($C_{5,5'}$,$_{7,7'}$), 159.971 (C=O) ($C_{3,3'}$), 208.12 (C =S) ($C_{1,1'}$) (see, Figure 1 B).

(2) Synthesis of macrocyclic complexes via a one-pot reaction

An excess of KOH (3eq) was added with stirring to a solution of the secondary amine in MeCN/H_2O mixture (9:1). Carbon disulfide (2.8 equivalents) was added to the solution, and the mixture was stirred for 10 minutes allowing the formation of the potassium dithiocarbamate salt. The complex was prepared *in situ* (ligand salt was not isolated) by the addition of one equivalent of the metal ion. The mixture was stirred overnight, water was added for precipitation if required, filtered and dried to give the macrocyclic complex. Analytical data are similar to that complexes obtained from the free ligand approach.

RESULTS AND DISCUSSION

Chemistry

The reaction of carbon disulfide with secondary bis-amines in the presence of KOH resulted in the formation of the free ligands (L^1 and L^2), see Scheme (1). The ligands were characterised by elemental analysis (TABLE 1), FTIR (TABLE 2), UV–Vis (TABLE 3), mass and ^{1}H, ^{13}C NMR spectroscopy. The formation

TABLE 1 : Colours, yields, melting points and (C, H, N, S) analysis, and values for ligands and bis(dithiocarbamate)-based complexes

Metal ion	Molecular formula	Colour	m.p. °C	Yield (%)	Found (Calca%)					Cl
					M%	C	H	N	S	
L^1	$C_{30}H_{34}Cl_2K_2N_4O_2S_4$	Light yellow	188 - 190	66	-	46.56 (47.41)	4.21 (4.51)	7.82 (7.37)	16.26 (16.88)	9.11 (9.33)
$[Mn(L^1)]_2$	$C_{60}H_{68}Cl_4N_8O_4S_8Mn_2$	Brown	242	42.85	7.22 (7.46)	48.08 (48.91)	4.33 (4.65)	7.95 (7.6)	17. 18 (17.41)	9.55 (9.62)
$[Co(L^1)]_2$	$C_{60}H_{68}Cl_4N_8O_4S_8Co_2$	Dark green	255	50	-	-	-	-	-	-
$[Ni(L^1)]_2$	$C_{60}H_{68}Cl_4N_8O_4S_8Ni_2$	Green	286	46.15	7.42 (7.93)	48.15 (48.66)	4.07 (4.63)	6.85 (7.57)	17.21 (17.32)	9.05 (9.58)
$[Cu(L^1)]_2$	$C_{60}H_{68}Cl_4N_8O_4S_8Cu_2$	Brown	278	41.02	-	-	-	-	-	-
$[Zn(L^1)]_2$	$C_{60}H_{68}Cl_4N_8O_4S_8Zn_2$	Palee yellow	256	44.87	-	-	-	-	-	-
$[Cd(L^1)]_2$	$C_{60}H_{68}Cl_4N_8O_4S_8Cd_2$	Pale yellow	263	44.57	13.82 (14.15)	45.11 (45.37)	4.07 (4.63)	7.85 (7.05)	16.09 (16.15)	8.25 (8.93)
L^2	$C_{24}H_{26}Cl_2K_2N_4O_2S_4$	Light orange	173 - 175	61.41	-	41.40 (42.40)	3.83 (3.85)	7.09 (8.24)	18.49 (18.87)	9.98 (10.43)
$[Mn(L^2)]_2$	$C_{48}H_{52}Cl_4N_8O_4S_8Mn_2$	Brown	275	46.75	-	-	-	-	-	-
$[Co(L^2)]_2$	$C_{48}H_{52}Cl_4N_8O_4S_8Co_2$	Light brown	270	42.85	8.23 (8.92)	43.50 (43.64)	3.10 (3.97)	8.63 (8.48)	19.37 (19.42)	9.68 (10.73)
$[Ni(L^2)]_2$	$C_{48}H_{52}Cl_4N_8O_4S_8Ni_2$	Dark green	285	46.75	-	-	-	-	-	-
$[Cu(L^2)]_2$	$C_{48}H_{52}Cl_4N_8O_4S_8Cu_2$	Dark brown	272	42.3	9.18 (9.55)	43.00 (43.33)	3.25 (3.94)	8.73 (8.42)	19.19 (19.28)	9.84 (10.66)
$[Zn(L^2)]_2$	$C_{48}H_{52}Cl_4N_8O_4S_8Zn_2$	Yellow	320	44.87	9.32 (9.80)	43.07 (43.21)	3.62 (3.93)	8.71 (8.40)	19.04 (19.23)	10.18 (10.63)
$[Cd(L^2)]_2$	$C_{48}H_{52}Cl_4N_8O_4S_8Cd_2$	Pale yellow	260	40.47	-	-	-	-	-	-

dithiocarbamate-based macrocyclic complexes were obtained either via a one-pot approach or from the reaction of the free ligand with a metal ion. In the later, the method was based on heating 1 mmole of the ligand with 1 mmole of metal chloride, using a mixture of MeCN/H_2O, see Scheme (2). The aim of this work is to obtain macrocyclic complexes in which the metal ion plays a key role in the self-assembly. All attempts to isolate crystals suitable for X-ray single crystal diffraction analysis were unsuccessful. The complexes are air-stable solids, soluble only in hot DMSO with stirring, and not soluble in other common organic solvents. Spectroscopic analyses were used to predict geometries about metal centres. The analytical data

TABLE 2 : FTIR spectral data (wave number) cm^{-1} of ligands and their complexes

Comp.	$_{Ami,}\nu$(N-H)	ν_{ar}(C-H)	ν_{ali}(C-H)	ν(C=O)	δ(NH)	ν_{ar}(C=C)	ν (NCS_2)	$\nu_{as,s}(CS_2)$	νC-Cl	νM-S
L^1	3299	3086	2922, 2844	1676	1622	1545	1441	1084, 976	654	-
$[Mn(L^1)]_2$	3293	3095	2933, 2850	1682	1628	1550	1498	1151, 980	768	-
$[Co(L^1)]_2$	3249	3010	2939, 2850	1650	1514	1494	1488	1090, 980	798	-
$[Ni(L^1)]_2$	3224	3012	2931, 2848	1656	1512	1446	1454	1070, 984	667	389, 374
$[Cu(L^1)]_2$	3265	3005	2927, 2856	1644	1576	1520	1452	1105, 933	752	-
$[Zn(L^1)]_2$	3290	3010	2927, 2850	1685	1612	1550	1498	1078, 976	773	-
$[Cd(L^1)]_2$	3296	3010	2922, 2856	1628	1550	1498	1452	1084, 980	773	385
L^2	3259	3032	3933	1643	1529	1498	1406	1001, 885	706	-
$[Mn(L^2)]_2$	3243	3032	29,222,856	1641	1550	1504	1441	1115, 949	712	-
$[Co(L^2)]_2$	3294	3037	2912, 2844	1666	1599	1520	1440	1059, 980	646	383,368
$[Ni(L^2)]_2$	3250	3016	2927, 2850	1689	1514	1446	1416	1068, 980	665	-
$[Cu(L^2)]_2$	3252	3037	2918	1645	1606	1523	1498	1001, 980	721	-
$[Zn(L^2)]_2$	3271	3030	2927, 2852	1636	1527	1500	1426	1073, 995	723	397,378
$[Cd(L^2)]_2$	3265	3032	2922, 2856	1649	1612	1529	1493	1001, 885	721	-

(TABLE 1) agree well with the suggested formulae. The important infrared bands of the ligands and their complexes together with their assignments are collected in (TABLE 2). The electronic spectra for the ligands and their complexes are presented in (TABLE 3).

FTIR and NMR spectra

The FTIR spectral data is collected in TABLE (2). FTIR spectra of L^1 and L^2 exhibit bands around 3299-3259 cm^{-1} due to ν(N–H) stretching. Band related to ν(C=O) amide is observed at 1676 and 1643 cm^{-1} for L^1 and L^2, respectively. Bands assigned to $\nu_{as}(CS_2)$ and $\nu_s(CS_2)$ functional groups were observed at 1084, 1001 and 976, 885 cm^{-1} for L^1 and L^2, respectively. Peaks related to ν(C-Cl) detected at 654 and 706 cm^{-1} for L^1 and L^2, respectively (see supporting information, Figures SI 18 and 22). Evidence for the formation of dinuclear-macrocyclic complexes was deduced from their FTIR spectra. Bands at 1420-1498 cm^{-1} that resulted from the stretching of the *C-N*-S bond indicated a partial delocalization of π-electron density within the dithiocarbamate moieties[21]. Peaks detected at 1001-1151 cm^{-1} and 933-995 cm^{-1} were assigned to $\nu_{as}(CS_2)$ and $\nu_s(CS_2)$, respectively. This is in accordance with an anisobidentate chelation mode of the ligand to the metal atoms[22,23]. Complexes exhibited two sets of bands around 368-397cm^{-1}, which are assigned to the ν(M-S) vibration mode, and supporting the anisobidentate chelation mode of the ligand[9] (see supporting information, Figures SI 19-21 and 23, 24). The ^1H and ^{13}C NMR spectra of the ligands displayed signals corresponding to the various protons and carbon nucleus indicating the formation of the ligands (See Experimental section). The ^1H NMR spectra DMSO-d_6 solution of the ligands show peaks at ca. 5.00 ppm assigned to CH ($C_{2,2}$'-*H*). The downfield appearance of this signal may due to attachment to withdrawing groups (C=O, N-H and Cl). The $_{ami}$(N-*H*) signal for the amide moiety appears as singlet at its expected resonance around 8.50 ppm (see supporting information, Figures SI 14 and SI 15)). The ^{13}C NMR spectrum DMSO-d_6 solution of L^1 and L^2 show a chemical shift of the carbonyl moiety at δ= 160.33 and 163.26 ppm in L^1 and L^2, respectively. The formation of the free ligands has been supported by detecting signals around δ=189.87 and 190.34 ppm, which attributed to quaternary carbon in dithiocarbamate moiety C=S in L^1 and L^2, respectively (see, Figure 1A for L^1 and supporting information, Figure SI 16). The ^1H-NMR spectrum for $[Cd(L^1)]_2$ in DMSO-d_6 solution displays the $_{ami}$(N-H) signal for the amide moiety at δ= 8.19 ppm, confirming the non-involvement of the amide group upon complexation[24] (see, Figure 1A for L^1 and supporting information, Figure SI 14). The ^{13}C NMR spectra of $[Cd(L^1)]_2$ exhibits a number of different carbons in a molecule with the appropriate shifting, compared with that in the free ligand, indicating the formation of the Cd-complex. The chemical shift for C=S moiety is detected at 208.12 ppm in $[Cd(L^1)]_2$, compared with that at 189.87 in the free ligand confirming the involvement of this moiety in complexation[25] (see Figure (1)).

Mass spectra

The electrospray (+) mass spectrum of $[Zn(L^1)]_2$ complex. The parent ion peak is not observed upon fragmentation for $C_{60}H_{68}Cl_4N_8O_4S_8Zn_2$, requires1494.39. Peaks detected at m/z=1307.3 (9%), 1062.8 (9 %) 748.2 (19 %), 560.8 (8 %) and 245.3 (10 %) related to $[M-(NH-CO-CHCl-(N-C_6H_{11}))]^+$, $[M-(NH-CO-CHCl-(N-C_6H_{11}))+((Ph)_2NH-CO-CHCl)]^+$, $[M-(NH-CO-CHCl-(N-C_6H_{11}))+((Ph)_2NH-CO-CHCl)+((N-C_6H_{11})(CS_2)_2Zn)]^+$, $[M-(NH-CO-CHCl-(N-C_6H_{11}))+((Ph)_2NH-CO-CHCl)((N-C_6H_{11})+(CS_2)_2Zn)+(NH-CO-CHCl-(N-C_6H_{11}))]^+$ and $[M-(NH-CO-CHCl-(N-C_6H_{11}))+((Ph)_2NH-CO-CHCl)+((N-C_6H_{11})+(CS_2)_2Zn)+(NH-CO-CHCl-(N-C_6H_{11})+((N-C_6H_{11})+(CS_2)_2Zn)]^+$ (see supporting information, Figure SI 6). The electrospray (+) mass spectrum of $[Zn(L^2)]_2$ complex showed no parent ion peak upon fragmentation, for $C_{48}H_{52}Cl_4N_8O_4S_8Zn_2$, requires 1334.10. Peaks detected at m/z=891.6 (5%), 667.8 (7 %), 449.1 (32 %) and 301.3 (3 %) related to $[M-((Ph)_2NH-CO-CHCl-N-C_3H_7CS_2Zn)]^+$, $[M-((Ph)_2NH-CO-CHCl-N-C_3H_7CS_2Zn)+(NH-CO-CHCl-N-C_3H_7CS_2)]^+$, $[M-((Ph)_2NH-CO-CHCl-N-C_3H_7CS_2Zn)+(NH-CO-CHCl-N-C_3H_7CS_2)+(CS_2)_2Zn)]^+$and $[M-((Ph)_2NH-CO-CHCl-N-C_3H_7CS_2Zn)+(NH-CO-CHCl-N-C_3H_7CS_2)+((CS_2)_2Zn)+(NH-CO-CHCl-N-C_3H_7)]^+$ (see supporting information, Figure SI 7).

TABLE 3 : UV-Vis spectral data of ligands and bis(dithiocarbamate)-based complexes in DMSO solutions, molar conductance and magnetic moment

Comp.	Band Position λ_{nm}	Wave number (cm^{-1})	Extinction coefficient ε_{max} ($dm^3 mol^{-1} cm^{-1}$)	Assignment	Λ_M($\Omega^{-1}cm^2mol^{-1}$)	μ_{eff} (B.M)
L^1	268 342 359	37313 41322 27855	1239 2247 1280	Intra-ligand $\pi \rightarrow \pi^*$ $n \rightarrow \pi^*$	-	-
$[Mn(L^1)]_2$	267 324 432	37458 30864 23148	884 393 77	Intra-ligand $\pi \rightarrow \pi^*$ C.T $^6A_1 \rightarrow {}^4T_1$	19.9	5.76
$[Co(L^1)]_2$	268 328 670	37313 30487 14925	1028 1613 44	Intra-ligand $\pi \rightarrow \pi^*$ C.T $^4A_2{}^{(F)} \rightarrow {}^4T_1{}^{(p)}$	8.47	3.72
$[Ni(L^1)]_2$	265 343 478 645	37735 29154 20920 15503	1223 2501 455 187	Intra-ligand $\pi \rightarrow \pi^*$ C.T $^1A_1g^{(F)} \rightarrow {}^1B_1g^{(F)}$ $^1A_1g^{(F)} \rightarrow {}^1A_2g^{(F)}$	5.86	Diamagnetic
$[Cu(L^1)]_2$	266 321 721 835	37593 31152 13869 11976	740 669 18 16	Intra-ligand $\pi \rightarrow \pi^*$, C.T $^2B_1g \rightarrow {}^2B_2g$ $^2B_1g \rightarrow {}^2A_2g$	9.77	1.41
$[Zn(L^1)]_2$	267 339	37458 29498	1226 2419	Intra-ligand $\pi \rightarrow \pi^*$, $n \rightarrow \pi^*$ C.T	3.72	Diamagnetic
$[Cd(L^1)]_2$	267 330	37458 30303	976 1795	Intra-ligand $\pi \rightarrow \pi^*$, $n \rightarrow \pi^*$ C.T	2.09	Diamagnetic
L^2	267 342	37453 41322	949 1032	Intra-ligand $\pi \rightarrow \pi^*$ $n \rightarrow \pi^*$	-	-
$[Mn(L^2)]_2$	297 320 370 430	33670 31250 27027 23255	1610 1430 1100 631	Intra-ligand $\pi \rightarrow \pi^*$ $n \rightarrow \pi^*$ C.T $^6A_1 \rightarrow {}^4T_1$	4.52	5.38
$[Co(L^2)]_2$	267 357 609	37453 28011 16420	1111 774 121	Intra-ligand $\pi \rightarrow \pi^*$, $n \rightarrow \pi^*$ C.T $^4A_2{}^{(F)} \rightarrow {}^4T_1{}^{(p)}$	3.84	3.50
$[Ni(L^2)]_2$	285 371 412	35087 26954 24271	2123 915 611	Intra-ligand $\pi \rightarrow \pi^*$, $n \rightarrow \pi^*$ C.T $^1A_1g^{(F)} \rightarrow {}^1B_1g^{(F)}$	5.76	Diamagnetic
$[Cu(L^2)]_2$	268 385 608 671	37313 25974 16447 14903	740 994 149 159	Intra-ligand $\pi \rightarrow \pi^*$, $n \rightarrow \pi^*$ C.T $^2B_1g \rightarrow {}^2B_2g$ $^2B_1g \rightarrow {}^2A_2g$	14.49	1.26
$[Zn(L^2)]_2$	268 342	37313 41322	786 2055	Intra-ligand $\pi \rightarrow \pi^*$, $n \rightarrow \pi^*$ C.T	4.56	Diamagnetic
$[Cd(L^2)]$	268 326	37313 30674	711 1301	Intra-ligand $\pi \rightarrow \pi^*$, $n \rightarrow \pi^*$ C.T	3.13	Diamagnetic

Full Paper

UV-Vis Spectral data for the complexes, and magnetic susceptibility

The electronic spectra of L^1 and L^2 in DMSO solutions revealed peaks at 267-359 nm assigned to $\pi \rightarrow \pi^*$ and $n \rightarrow \pi^*$ transitions, respectively [26-28], (see supporting information, Figures SI 25 and 29 and TABLE (3)). The electronic spectra of the complexes exhibited various extents of bathochromic shift of bands at 265-268 and 267-297 nm related to the ligand field $\pi \rightarrow \pi^*$ and $n \rightarrow \pi^*$ transitions in L^1 and L^2 complexes. Bands at 321-343 and 320-385 nm related to the charge transfer transitions (CT) in L^1 and L^2 complexes[29], (see supporting information, Figures SI 26-28 and 30, 31). The spectrum of the Mn(II)-complex showed a peak in the d-d region at 432 nm assigned to $^6A_1 \rightarrow {}^4A_1$ transition, indicating tetrahedral geometry about Mn(II) ion[30,31], (see supporting information, Figure SI 26). The magnetic moment value 5.76 B.M of $[Mn^{II}(L^1)]_2$ is typical for a high spin Mn(II) ion, which assigned to tetrahedral structures for Mn(II)-complexes[30,32]. The Co(II) complex exhibits an additional peak in the d-d region at 670 nm due to $^4A_2{}^{(F)} \rightarrow {}^4T_1{}^{(p)}$ transitions, indicating tetrahedral geometry around Co atom[31,32], (see supporting information, Figure SI 27). The μ_{eff} value of 3.72 B.M for Co-complex confirms the formation of a four-coordinate complex with a tetrahedral arrangement about metal centre[30,32]. The spectrum of the Ni(II)-complex displayed peaks in the d-d region at 478 and 645 nm assigned to $^1A_1g^{(F)} \rightarrow {}^1B_1g^{(F)}$ and $^1A_1g^{(F)} \rightarrow {}^1A_2g^{(F)}$, respectively indicating square planar geometry about Ni atom[31,32]. The magnetic moment measurement for $[Ni^{II}(L^1)]_2$ complex reveals a diamagnetic arrangement. The experimental magnetic value of Ni(II) complex along with other analytical data indicated square planar geometry about Ni atom. The spectrum of the Cu(II)-complex exhibited peaks in the d-d region at 721 and 835 nm attributed to d-d transitions type $^2B_1g \rightarrow {}^2B_2g$ and $^2B_1g \rightarrow {}^2A_2g$, respectively confirming square planar geometry about Cu atom[29-31], (see supporting information, Figure SI 28). The magnetic moment value of 1.41 B.M for $[Cu^{II}(L^1)]_2$ complex confirms the square planar geometry around Cu(II) ion[30,31]. The electronic spectra of the $[Zn(L^1)]_2$ and $[Cd(L^1)]_2$ complexes exhibited peaks at 267, 267 and 339, 330 nm that assigned to the ligand field and charge transfer transitions in Zn- and Cd-complex, respectively[28,29]. The spectra of the Mn(II), Co(II), Ni(II), Cu(II), Zn(II) and Cd(II) complexes of L^2 showed similar behaviour to those of L^1, suggesting tetrahedral geometries for Mn(II), Co(II), Zn(II) and Cd(II), and square planar geometries with Ni(II), (see supporting information, Figure SI 30) and Cu(II) complexes. The molar conductance of the complexes in DMSO solutions is indicative of their non-electrolytic nature[33,34], see TABLE (1). The electronic data, molar conductance and magnetic moment measurements of L^1 and L^2 complexes with their assignments are listed in (TABLE 3).

Thermal analysis

Thermal properties of the ligands and some metal complexes are summarised in TABLE (4). The TG-DSC curves of the ligands and their complexes were measured from ambient temperature up to 600 °C in the atmosphere of nitrogen. The analysis of thermal data showed ligand L^1 is stable up to 85 °C with a weight loss of 15.87%, which attributed to (KCS_2) fragment. The peak detected at 128-238ºC related to the (diphenyl-NCOCHClNphenyl+C+CS_2) segment with 63.85% weight loss. The third step occurs at 240-590ºC is related to the loss of (C_2H_2) fragments with a weight loss of 3.50%. This peak accompanied by an endothermic behaviour in the DSC curve at 574.4 °C. The final residue of the compound is related to the (phenyl-CHOCl) with 12.26% weight loss (see supporting information, Figure SI 32). Thermal data showed L^2 is stable up to 138 °C with weight loss 20.93% that attributed to (CS_2NCHCl) segment. The second step at 282-500 ºC attributed to the loss of (SO) molecules, with a weight loss of 7.29%. This peak is indicated by an endothermic effect by the DSC at 485.5 °C. The final residue of the compound confirmed the mass loss of 77.40% that attributed to (CHN-diphenyl-HNCOCHClNCHCH$_3$CH$_3$, CS_2, 2K and CHCH$_3$CH$_3$), (see supporting information, Figure SI 35). The thermal data indicated that L^2 is thermally more stable than L^1. The thermal analysis properties of $[Mn(L^1)]_2$ (see supporting information, Figure SI 33), $[Co(L^1)]_2$, (see supporting information, Figure SI 34), $[Ni(L^1)]_2$, $[Cu(L^2)]_2$, (see supporting information, Figure SI 36), $[Zn(L^2)]_2$ (see supporting information, Figure

TABLE 4 : TGA/DTG and DSC data for ligands and complexes

Comp	Stable up to °C	Stage	Decomposition temperature initial-final °C	fragments	Nature of transformation/intermediate formed% mass found (calc.), mg	Nature of DSC peak and temp. °C	DTG peak temp. °C
L^1	85	1	85-125	(KCS_2)	2.3807 (2.2745)	85 Exo	-
		2	128-238	(diphenyl-NCOCHCl Nphenyl+C+CS_2)	9.5780 (9.4936)	132.2,173.3,215.0,404.7,483.8 Endo	-
		3	240-590	(C_2H_2)	0.5254 (0.5139)	574.4 Endo	-
$[Mn(L^1)]_2$	110	1	110-264	($2CH_2$ CH_2 CH_2 CH_2 CHNCHCl HN+ $HNCOCHClNCHCH_2CH_2$ CH_2 +$4CS_2$ +CHCONH)	5.1091 (5.0773)	120,185 Exo	-
		2	265-598	(Cl+CONH)	0.4753 (0.4288)	241, 400.6 Endo	-
$[Co(L^1)]_2$	105	1	105-218	($HNCOCHClNCHCH_2CH_2$ $CH_2CH_2CH_2$+ $4CS_2$+$CH_2CH_2CH_2CH_2$ CH_2CHNCH_2 CO +CHCOHN)	4.2179 (4.2117)	185.8 Endo	200
		2	220-560	(diphenyl-NHCONCHCl + $CH_2CH_2CH_2CH_2CH_2CH_2$)	2.0267 (2.0039)	455 Endo	-
$[Ni(L^1)]_2$	120	1	120-223	($HNCOCHClNCHCH_2CH_2CH_2CH_2CH_2$+ HNCOCH+$4CS_2$+$CH_2CH_2CH_2CH_2CH_2$CHN)	5.2707 (5.2669)	184.7 Endo	-
		2	225-598	($HNCOCHClNCHCH_2CH_2CH_2CH_2CH_2$+Cl)	1.8161 (1.8158)	520Endo	-
L^2	138	1	138-280	(CS_2NCHCl)	0.8372 (0.8215)	189.7 Exo	-
		2	282-500	(SO)	0.2919 (0.2830)	485Endo	-
$[Cu(L^2)]_2$	160	1	160-280	($2CS_2$ Cu+NCOCHClNH)	1.4423 (1.4537)	284 Endo	-
		2	282-350	(HN-diphenyl-$HNCOCHClNCHCH_3CH_3$)	1.4085 (1.4242)	350 Endo	-
		3	355-590	($2CS_2$)	1.0194 (1.1353)	580 Endo	-
$[Zn(L^2)]_2$	100	1	100-345	(CS_2 + CO+CH_2+$NCHCH_3CH_3$)	1.131 (1.4537)	175 Exo	-
		2	350-598	($CS_2ZnNCHCH_3CH_3$+$HNCOCHClNCHCH_3CH_3$+CS_2)	2.6550 (2.6339)	437.7 Endo	-
$[Cd(L^2)]_2$	140	1	140-305	(O+Cl)	0.5083(0.4683)	448.4 Endo	-
		2	308-495	(CS_2+CH Cl +$NCHCH_3CH_3$)	1.7374 (1.7908)	520 Endo	-

SI 37) and $[Cd(L^2)]_2$ complexes are listed in TABLE (4). Thermal data of $Mn(L^1)]_2$, $[Co(L^1)]_2$, $[Ni(L^1)]_2$, $[Zn(L^2)]_2$ and $[Cd(L^2)]_2$ complexes consists of two steps. The first step accompanied by exothermic behaviour as confirmed by the DSC at 120 and 175 °C for $[Mn(L^1)]_2$ and $[Zn(L^2)]_2$, respectively. However, $[Co(L^1)]_2$, $[Ni(L^1)]_2$, $[Cu(L^2)]_2$ and $[Cd(L^2)]_2$ complexes exhibit an endothermic peaks at 185.5, 184.7, 284 and 448°C, respectively. The weight loss and other thermal properties including lost fragments of

Full Paper

TABLE 5 : Biological activity of ligands and bisdithiocarbamate-based complexes

No.	Sample	Average inhibition zone (mm)			
		E.coli	*P.aeruginosa*	*B.sabtuius*	*S.aureus*
1	L^1	6	5	5	3
2	$[Mn(L^1)]_2$	12	11	13	15
3	$[Co(L^1)]_2$	13	12	16	15
4	$[Ni(L^1)]_2$	12	13	12	12
5	$[Cu(L^1)]_2$	10	12	9	10
6	$[Zn(L^1)]_2$	-	-	13	11
7	$[Cd(L^1)]_2$	12	17	25	16
8	L^2	2	5	9	7
9	$[Mn(L^2)]_2$	18	14	11	10
10	$[Co(L^2)]_2$	18	18	13	15
11	$[Ni(L^2)]_2$	11	12	14	12
12	$[Cu(L^2)]_2$	15	10	-	-
13	$[Zn(L^2)]_2$	12	13	17	12
14	$[Cd(L^2)]_2$	22	10	21	20

the complexes are listed in TABLE (4),[35,36].

Bacterial activity

Dithiocarbamate ligands and their metal complexes were tested for their antimicrobial activity against four bacterial species (*Escherichia coli, Pseudomonas aeruginosa* (G-), *Staphylococcus aureus and Bacillus stubtilis* (G+)). The role of DMSO in the biological activity was clarified by separate studies carried out with the solutions of DMSO alone, which showed no activity against any bacterial strains[37]. The measured zones of inhibition against the growth of different microorganisms are listed in TABLE (5). Biological data showed that complexes become potentially more active against these bacterial strains (except $[Zn(L^1)]_2$ with *E. coli* and, *P. aeruginosa* and $[Cu(L^2)]_2$ with *B. sabtuius* and *S. aureus*) compared with the free ligands (see Figure 2). This may be explained by chelation effect in which the partially sharing of the positive charge of the metal in complexes by the donor atoms present in the ligand and there may be π-electron delocalization over the whole chelate ring that increases the lipophilic character of the metal chelate system. This will favour its permeation through lipid layer of the cell membranes [38,39]. From the obtained data that listed in TABLE (5), L^2 complexes are more active against these bacterial strains compared with L^1 complexes and Cd-complexes almost has the higher antimicrobial activity compared

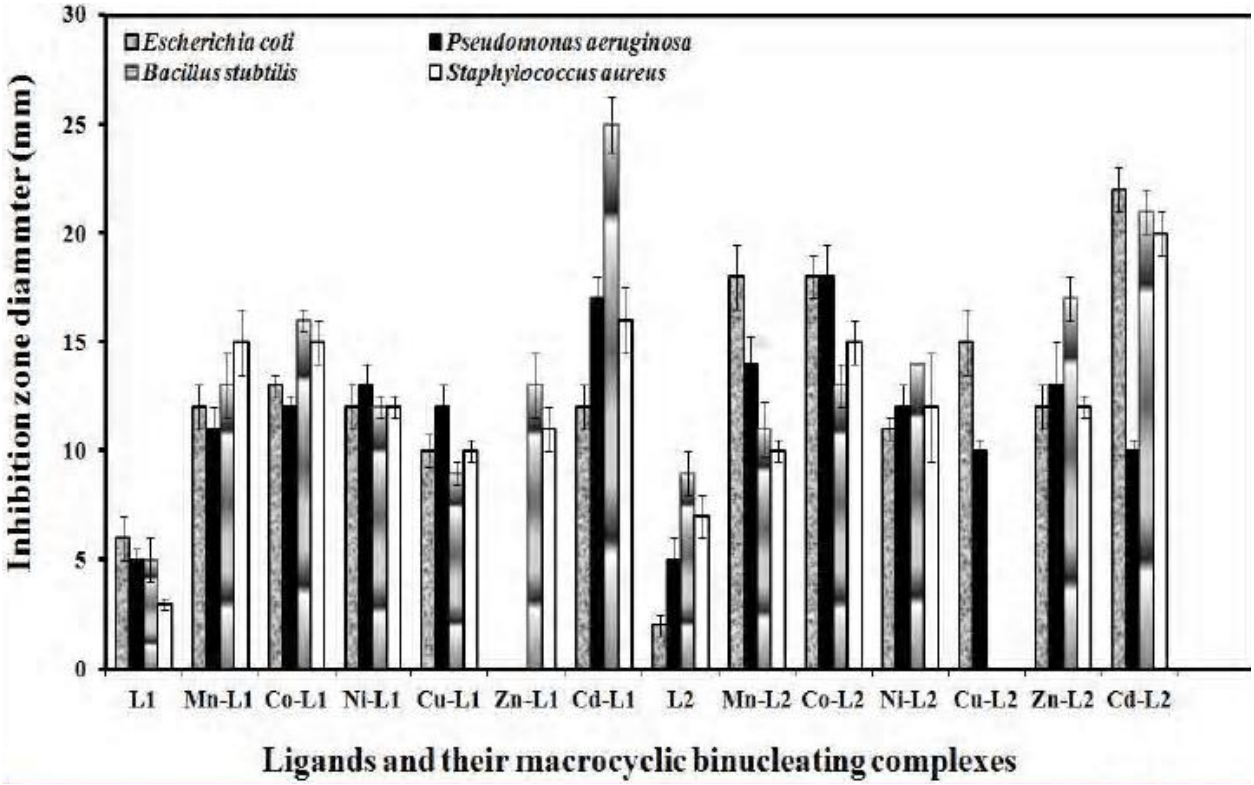

Figure 2 : Evolution of diameter zone (mm) of inhibition of L^1, L^2 and their bimetallic complexes against the growth of various microorganisms. Error bars represent SD between repeated tests.

with the other complexes. This may be related to the size of Cd^{II} ion and/or its softer character, compared with other metal ions in complexes.

CONCLUSION

The formation of new bimetallic dithiocarbamate macrocyclic complexes is reported. The synthesis of these complexes was achieved using two approaches; (i) from the reaction of the free ligand with a metal ion, or (ii) via a one-pot reaction. In these complexes, the metal ion plays a key role in the self-assembly. The mode of bonding and overall structure of the complexes were determined by physico-chemical and spectroscopic methods. These results indicated the formation of four-coordinate complexes in the solid state and in solution. Biological activities revealed that complexes found to be potentially more active against these bacterial strains, compared with the free ligands.

REFERENCES

[1] P.D.Beer, N.G.Berry, A.R.Cowley, E.J.Hayes, E.C.Oates, W.W.H.Wong; Chem.Commun., **19**, 2408–2409 **(2003)**.
[2] H.Nabipour, S.Ghammamy, S.Ashuri, Z.S.Aghbolaghc; J.Org.Chem., **2**, 75-80 **(2010)**.
[3] A.F.M El Walily, O.A.Razak, S.F.Belal, R.S.Bakry; J.Pharm.Biomed Anal., **21(2)**, 439–449 **(1999)**.
[4] P.Figueira, C.B.Lopes,A.L.Danieli-da-silva, E.C.P.Duarte, T.Trindad; Water Res., **45**, 17, 5773-5784 **(2011)**.
[5] S.Singh, N.Bhattacharya, Subrato; J.Organomet. Chem, **700**, 69-77 **(2012)**.
[6] C.Marzano,L.Ronconi, F.Chiara, M.C.Giron, I.Faustinelli, P.Cristofori, A.Trevisan, D.Fregona; Int.J.Cancer., **129**, 2, 487-496 **(2011)**.
[7] E.Amin, A.A.Saboury, H.Mansuri-Torshizi, A.A.J.Moosavi-Movahedi; Enzyme Inhib.Med.Chem., **25**, 2, 272-281 **(2010)**.
[8] G.Hogarth; Metal-dithiocarbamate complexes: chemistry and biological activity., **12**, 12, 1202-15 **(2012)**.
[9] H.A.Hasan, E.I.Yousif, M.J.Al-Jeboori; Global J.Inorg.Chem, **3**, 10, 1-7 **(2012)**.
[10] C.Bolzati, E.Benini, M.Cavazza-Ceccato, E.Cazzola, E.Malago, S.Agostini, F.Tisato, F.Refosco, G.Bandoli; Bioconjug Chem, **17**, 2, 419-28 **(2006)**.
[11] C.Bolzati, A.Boschi, L.Uccelli et al.; J.Am.Chem.Soc., **124**, 38, 11468–11479 **(2002)**.
[12] R.N.Goyal, A.A.Umar, M.Oyama; J.Electro. Chem., **631**, 1-2, 58–61 **(2009)**.
[13] P.B.Hitchcock, A.G.Hulkes, M.F.Lappert, Z.Li; Dalton Trans., **1**, 129-36 **(2004)**.
[14] A.Normah,N.Farahana, B.Ester, H.Asmah, N.Rajab, A.Halim; Res.J.Chem.Environ., **15**, 544-549 **(2011)**.
[15] H.Tlahuext, R.Reyes-Martinez, G.Vargas-Pineda, M.Lopez-Cardoso, H.Hopfl; J.Organomet.Chem., **696**, 693-701 **(2011)**.
[16] A.Tlahuext-Aca1, H.Hopfl, F.Medrano-Valenzuela, J.Guerrero-Alvarez, H.Tlahuext, K.O.Lara, V.Reyes-Márquez, M.Tlahuext; Inorg.Chem., **638**, 11,1731–1738 (2012).
[17] M.D.Pratt, P.D.Beer; Tetrahedron, **60**, 49, 11227–11238 **(2004)**.
[18] J.Cookson, E.A.L.Evans, J.P.Maher, C.Serpell, R.P.Paul, A.R.Cowley, M.Drew, P.D.Beer; Inorg.Chimica Acta., **363**, 6, 1195-1203 **(2010)**.
[19] G.Faraglia, S.Sitran, D.Montagner; Inorg.Chim.Acta., **358**, 971-980 **(2005)**.
[20] M.J.Al-Jeboori, F.A.Al-Jeboori, M.A.R.Al-Azzawi; Inorg.Chim.Acta., **379**, 1, 163-170 **(2011)**.
[21] B.F.Johnson, K.H.Al-Obalidi, J.A.Mecleverty; J.Chem.Soc.A., **19**, 1668-1670 **(1969)**.
[22] G.R.Fulmer, A.J.M.Miller, N.H.Sherden, H.E.Gottlieb, A.Nudelman, B.M.Stoltz, J.E.Bercaw, K.I.Goldberg; Organomet., **29**, 9, 2176-2179 **(2010)**.
[23] S.Srinivasan, K.Ramalingam, C.Rizzoli, Synthesis; Polyhedron., **33**, 1, 60-66 **(2012)**.
[24] V.Orescanin, L.Mikelic, V.Roje, S.Lulic; Analytical Chimica Acta., **570**, 2, 277-282 **(2006)**.
[25] R.N.Jowitt, P.C.H.Mitchell; J.Chem.Soc.part A., 1702-1708 **(1970)**.
[26] L.Ronconi, L.Giovagnini, C.Marzona, F.Bettio, R.Graziani,G.Pilloni, D.Fregona; Inorg.Chem., **44**, 6,1867-1881 **(2005)**.
[27] P.K.Pandey, A.K.Pandey, A.N.Mishra, K.K.Ojha, S.R.Kumar; Indian J.Sci.Res., **3**, 1, 119-122 **(2012)**.
[28] M.J.Al-Jeboori, H.H.Al-Tawel, R.M.Ahmad; Inorg.Chimica Acta., **363**, 6, 1301-1305 **(2010)**.
[29] K.S.Siddiqi, S.A.A.Nami, Lutfullaha,Y.Chebudeb; J.Braz.Chem.Soc., **17**, 1, 107-112 **(2006)**.
[30] M.Du, X.H.Bu, Y.M.Guo, J.Ribas; J.Chem., **10**,

1345 **(2004)**.
[31] S.M.Mamba, A.K.Mishara, B.B.Mamba, P.B.Njobeh, M.F.Dutton, E.Fosso-Kankeu; Spectrochimica Acta part A., **77**, 3, 579-587 **(2010)**.
[32] K.Slddappa, K.Mallikarjun, T.Reddy, M.Mallikarjun, C.Vreddy, M.Tambe; E-Journal of Chemistry., **6**, 3, 615-624 **(2009)**.
[33] E.Canpolat, M.Kaya; J.Coord.Chem., **31**, 7511-515 **(2005)**.
[34] W.J.Geary; J.Coord.Chem.Rev., **7**, 81-122 **(1971)**.
[35] C.Qing, Z.Ming-Hua, W.Lian-Qiang, K.Mohamedally; Chem.Mater., **22**, 4328-4334 **(2010)**.
[36] A.Rahman, M.Choudhary, W.Thomsen; Bioassay Techniques For Drug Development, Harwood Academic.Amsterdam, **(2001)**.
[37] A.Himanshu, L.Francesc, M.Rabindranath; Eur.J.Inorg.Chem., **22**, 3317-3325 **(2009)**.
[38] R.V.Singh, R.Dwivedi, S.C.Joshi; Trans.Met.Chemi., **29**, 1, 70–74 **(2004)**.
[39] B.G.Tweedy; Phytopathology., **55**, 910–914 **(1964)**.